

# Static dielectric properties of dense ionic fluids

Grigory Zarubin\* and Markus Bier†

*Max-Planck-Institut für Intelligente Systeme, Heisenbergstr. 3,  
70569 Stuttgart, Germany, and Institut für Theoretische Physik IV,  
Universität Stuttgart, Pfaffenwaldring 57, 70569 Stuttgart, Germany*

(Dated: 28 April 2015)

The static dielectric properties of dense ionic fluids, e.g., room temperature ionic liquids (RTILs) and inorganic fused salts, are investigated on different length scales by means of grandcanonical Monte Carlo simulations. A generally applicable scheme is developed which allows one to approximately decompose the electric susceptibility of dense ionic fluids into the orientation and the distortion polarization contribution. It is shown that at long range the well-known plasma-like perfect screening behavior occurs, which corresponds to a diverging distortion susceptibility, whereas at short range orientation polarization dominates, which coincides with that of a dipolar fluid of attached cation-anion pairs. This observation suggests that the recently debated interpretation of RTILs as dilute electrolyte solutions might not be simply a yes-no-question but it might depend on the considered length scale.

## I. INTRODUCTION

Room-temperature ionic liquids (RTILs) have become an extensively investigated topic in recent years. RTILs are salts with melting points at about room temperature, in contrast to inorganic salts such as NaCl with a melting point of 1081 K [1]. The first report of an RTIL is dated to 1914, when the compound ethylammonium nitrate with a melting temperature of 285 K was synthesized [2]. Since the 1990s interest in RTILs has grown greatly due to the discovery of a huge number of air- and water-stable compounds (see, e.g., Ref. [3] and the references therein).

Besides the strikingly low melting point, RTILs exhibit a number of remarkable general, i.e., material-independent, physical properties such as an extremely low vapour pressure [4, 5] and a high viscosity at ambient temperature — the lowest viscosity of RTILs at 298 K observed by now, 21 cP for [C<sub>2</sub>mim][N(CN)<sub>2</sub>] [6], is more than twenty times that of water. All these properties are related to the combination of strong electrostatic and highly anisotropic steric forces.

An interesting feature of the RTILs for applications is the high sensitivity of some physical properties on the choice of the cation and the anion. For example the viscosity of [C<sub>4</sub>mim][BF<sub>4</sub>] is only half of that of [C<sub>4</sub>mim][PF<sub>6</sub>] even though these RTILs differ only in the size of the (spherical) anions [7]. Therefore exploration of RTILs on the molecular level is crucial, in order to being able to “design” salts with prescribed properties. Computer simulations are frequently used as a tool, but the challenge is to find an adequate description of the interaction potentials. Such interaction potentials are complicated and depend upon many parameters (e.g., bond, angle and torsion parameters as well as van der Waals terms [8]). However, the aim of the present work is not

to model a specific RTIL with all its peculiarities but to investigate ionic fluids, i.e., RTILs and fused salts, from a general point of view which considers them mostly as fluids being composed of ions at high densities. Hence, since general features are expected to occur in all systems, one can focus on the simple system of equally-sized charged hard spheres, which is commonly called the restricted primitive model (RPM).

As RTILs are used as solvents in chemical studies, their polarity is one of the most important characteristics because it describes the global solvation capability of the solvent. In order to interpret surface force apparatus (SFA) measurements, it has been proposed recently [9] to view pure ionic liquids as dilute electrolyte solutions with a few mobile ions in an effective solvent made of temporarily paired ions. Whereas these SFA data have been doubted [10, 11], the interpretation of RTILs as dilute electrolyte solutions has attracted some interest [12]. For non-conducting fluids the static dielectric constant  $\epsilon$  is well defined and precisely measurable (see, e.g., Ref. [13, 14]). However, conducting fluids, such as ionic fluids, are well-known to perfectly screen external charges at *long* ranges [15, 16] so that the corresponding static dielectric constant is infinitely large. On the other hand, it is also well-known that cations and anions form a characteristic alternating pair structure at *short* ranges [15, 16], which, when considering neighboring cation-anion pairs, is analogous to the charge separation inside dipolar molecules. Therefore, it appears that the dielectric properties of dense ionic fluids depend on the length scale.

In the present work the analysis is based on the response of bulk ionic fluids to a static nonuniform electric field which spatially varies on a particular length scale. It has to be stressed that here the focus is on nonuniform static electric fields, the response onto which is described in terms of the wavenumber-dependent dielectric function  $\epsilon(k)$ , whereas numerous experimental studies consider uniform time-dependent fields, which give rise to the frequency-dependent dielectric function  $\epsilon(\omega)$  (see,

---

\* zarubin@is.mpg.de

† bier@is.mpg.de

e.g., [17–20]). Both quantities,  $\varepsilon(k)$  and  $\varepsilon(\omega)$ , are not easily related because the former describes the equilibrium structure whereas the latter quantifies the dynamics in uniform electric fields.

The dielectric properties of a substance can be interpreted in terms of two well-known mechanisms [21]: Orientation polarization refers to the rotation of dipolar moments upon keeping the magnitude constant, whereas distortion polarization describes the change of magnitude of dipolar moments at constant orientations. The according orientation susceptibility  $\chi_{\text{ori}}(k)$  and distortion susceptibility  $\chi_{\text{dis}}(k)$  both contribute to the total electric susceptibility  $\chi(k) = \varepsilon(k) - 1 = \chi_{\text{ori}}(k) + \chi_{\text{dis}}(k)$ . However, in order to infer the dominant polarization mechanism as a function of the wave number  $k$ , one has to somehow determine the decomposition of the observable  $\chi(k) = \varepsilon(k) - 1$  into the orientation and the distortion contribution. Perfect screening in ionic fluids and the according divergence  $\chi(k) \rightarrow \infty$  in the limit  $k \rightarrow 0$  [15, 16] corresponds to a dominating distortion polarization in the long-wavelength limit. This long-range behavior of ionic fluids is in sharp contrast to that of dipolar fluids, whose electric susceptibility  $\chi(k)$  attains a finite limit  $\chi(0)$  as  $k \rightarrow 0$ .

In order to achieve the decomposition of the electric susceptibility  $\chi(k)$  of an ionic fluid into the orientation and the distortion susceptibility  $\chi_{\text{ori}}(k)$  and  $\chi_{\text{dis}}(k)$ , respectively, the following approach is proposed: In addition to determine the electric susceptibility  $\chi(k)$  of the ionic fluid composed of cations and anions, a corresponding dipolar fluid is considered whose particles are overall charge-neutral dumbbells formed by gluing together pairs of cations and anions of the ionic fluid. This dipolar fluid does not exhibit distortion polarization, i.e.,  $\chi_{\text{dis}}(k) = 0$ , but only pure orientation polarization, i.e.,  $\chi(k) = \chi_{\text{ori}}(k)$ , and the latter can be expected to be similar to  $\chi_{\text{ori}}(k)$  of the corresponding ionic fluid at short ranges. The applicability of this approach is not restricted to the RPM investigated here but it can be used for any ionic fluid model.

A brief description of the theoretical methods as well as the considered models is given in Sec. II. The results of actual calculations are discussed in Sec. III from which general conclusions on the dielectric properties of ionic fluids are drawn in Sec. IV.

## II. MODELS AND METHODS

### A. Restricted primitive and dumbbell model

The model used to represent the ionic fluid is the three-dimensional restricted primitive model (RPM), i.e., a collection of  $N/2$  positively and  $N/2$  negatively charged hard spheres of equal diameter  $\sigma$  and equal absolute valencies  $|z_+| = |z_-|$  (see Fig. 1(a)). The interaction potential between two ions of species  $i$  and  $j$  with  $i, j \in \{+, -\}$

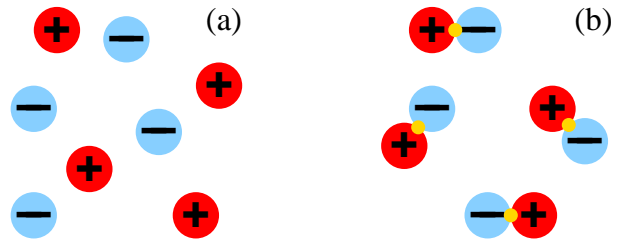


FIG. 1. Sketch of (a) the restricted primitive model (RPM) and (b) the corresponding dumbbell model (DM) with particles being constructed by pairwise gluing together oppositely charged hard spheres of the RPM.

at positions  $\mathbf{r}_i$  and  $\mathbf{r}_j$ , respectively, can be described as

$$\beta U_{ij}(\mathbf{r}_i, \mathbf{r}_j) = \begin{cases} \frac{z_i z_j l_B}{|\mathbf{r}_i - \mathbf{r}_j|} & , |\mathbf{r}_i - \mathbf{r}_j| \geq \sigma \\ \infty & , |\mathbf{r}_i - \mathbf{r}_j| < \sigma \end{cases} \quad (1)$$

with the vacuum Bjerrum length  $l_B = \beta e^2 / (4\pi \varepsilon_0)$ , where  $e$  is the elementary charge,  $\beta = 1/(k_B T)$  denotes the inverse temperature, and  $\varepsilon_0$  is the vacuum permittivity.

In this work, the dielectric properties of the RPM (see Fig. 1(a)) are compared with those of a corresponding dipolar fluid model whose particles are composed of one cation and one anion of the RPM glued together (see Fig. 1(b)). The particles within this dumbbell model (DM) possess three positional and two orientational degrees of freedom, in contrast to six translational degrees of freedom of a pair of ions within the RPM. Obviously, all configurations of  $N/2$  dumbbells correspond to possible configurations of the RPM with  $N/2$  positive and  $N/2$  negative hard spheres, but not all configurations of the RPM can be realized within the DM. The interaction energy between two dumbbell particles is given by the sum of contributions Eq. (1) of the constituent charged hard spheres.

### B. Dielectric properties

In this work the dielectric properties of ionic and dipolar fluids are studied by analyzing the linear response of the models introduced in the previous Subsec. II A in the presence of a weak static nonuniform external electric field. Within the linear response regime the dielectric properties are given by the dielectric function tensor  $\overleftrightarrow{\varepsilon}(\mathbf{k})$  or, equivalently, by the electric susceptibility tensor  $\overleftrightarrow{\chi}(\mathbf{k}) = \overleftrightarrow{\varepsilon}(\mathbf{k}) - 1$ . However, since electrostatic fields are purely longitudinal due to Faraday's law, the polarization field is also purely longitudinal in isotropic fluids. Therefore, only the longitudinal components (parallel to the wave vector  $\mathbf{k}$ )

$$\varepsilon(\mathbf{k}) := \varepsilon_{\parallel}(\mathbf{k}) = \frac{\mathbf{k} \cdot \overleftrightarrow{\varepsilon}(\mathbf{k}) \cdot \mathbf{k}}{k^2} \quad \text{and} \\ \chi(\mathbf{k}) := \chi_{\parallel}(\mathbf{k}) = \frac{\mathbf{k} \cdot \overleftrightarrow{\chi}(\mathbf{k}) \cdot \mathbf{k}}{k^2} = \varepsilon(\mathbf{k}) - 1 \quad (2)$$

are of relevance here.

It can be shown [22] that the longitudinal dielectric function  $\varepsilon(\mathbf{k})$  is related to the charge-charge structure factor

$$S_{zz}(\mathbf{k}) = \frac{1}{N} \left\langle \sum_m z_m \exp(-i\mathbf{k} \cdot \mathbf{r}_m) \sum_n z_n \exp(i\mathbf{k} \cdot \mathbf{r}_n) \right\rangle \quad (3)$$

via

$$\frac{1}{\varepsilon(\mathbf{k})} = 1 - \frac{4\pi l_B N}{\mathbf{k}^2 V} S_{zz}(\mathbf{k}). \quad (4)$$

In the present work the averaging in Eq. (3) is obtained by means of grandcanonical Monte Carlo simulations of the RPM and the DM.

### C. Grandcanonical Monte Carlo simulations

In order to determine the charge-charge structure factor  $S_{zz}(\mathbf{k})$  in Eq. (3), grandcanonical Monte Carlo simulations with Metropolis sampling [23–25] were performed in a cubic box of side length  $V^{1/3} = 10\sigma$  with periodic boundary conditions applying Ewald’s method [24–26]. In a first step, quick simulation runs were used to determine the relation between the chemical potential and the mean density  $N/V$  for fixed temperature. For calculation of the charge-charge structure factor  $S_{zz}(\mathbf{k})$  typically  $10^6 - 10^7$  relaxation and  $10^7 - 10^8$  evaluation steps were used. A Monte Carlo step involved a random selection of one of the following possible moves:

- translation of an ion (RPM) or of a dumbbell (DM) inside a small cube-like environment of size  $d^3$  with probability  $P_{\text{trans}}$ ,
- insertion of a cation and an anion (RPM) or of a dumbbell (DM) with probability  $(1 - P_{\text{trans}})/2$ , or
- removal of a cation and an anion (RPM) or of a dumbbell (DM) with probability  $(1 - P_{\text{trans}})/2$ .

Insertions and removals of charge-neutral entities guarantee global charge neutrality during the whole simulation. Values of  $P_{\text{trans}}$  and  $d$  were chosen in the way that the resulting rate of acceptance of the trial states did not drop below 30%. The Monte Carlo code has been validated by comparison to results obtained using the molecular dynamics package ESPResSo [27, 28].

## III. RESULTS AND DISCUSSION

In the present work the RPM (Sec. II A) is considered as a representative ionic fluid. Its dielectric function  $\varepsilon(\mathbf{k})$  is determined by using Eq. (4) via calculating the charge-charge structure factor  $S_{zz}(\mathbf{k})$ , Eq. (3), by means of grandcanonical Monte Carlo simulations

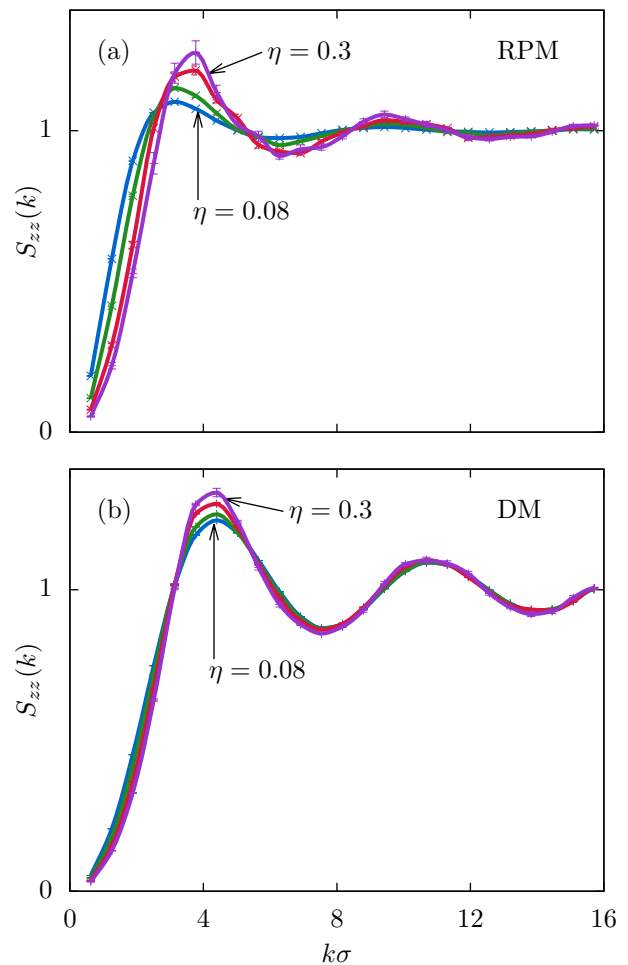


FIG. 2. Charge-charge structure factor of (a) the RPM (Sec. II A) and (b) the DM (Sec. II A) for the temperature  $T^* = 1$  and various values of the packing fraction  $\eta \in \{0.08, 0.14, 0.23, 0.3\}$ .

(see Subsec. II C). In the following discussion thermodynamic states are considered with the packing fractions  $\eta = \pi N \sigma^3 / (6V) \in [0.08, 0.33]$  and the temperatures  $T^* = \sigma / l_B \in [1/3, 1]$ . These conditions correspond to the plasma parameters  $\Gamma = 2\eta^{1/3} / T^* \in [0.86, 4.15]$ . Since the temperatures  $T^*$  are well above the critical temperature  $T_c^* \lesssim 0.1$  of the RPM [29], no influence of the vapor-liquid phase transition is expected to occur. Moreover,  $T^*$  is also well above the temperature range  $T^* \lesssim 1/4$ , where significant Bjerrum ion-pairing is expected to occur [29], which renders the RPM a dipolar fluid already in the gas phase. The high temperatures  $T^*$  used here allow one to study the crossover from plasma-like to dipolar-fluid-like behavior. The general trend of that crossover for varying  $\eta$  and  $T^*$  is captured by a simple approximative calculation described later.

Figures 2(a) and (b) display the charge-charge structure factors  $S_{zz}(\mathbf{k})$  of the RPM ionic fluid (Sec. II A) and of the DM (Sec. II A), respectively. The calculation was

performed several (5-10) times for each packing fraction separately, both for the RPM and the DM. This procedure allows one to calculate the mean value of  $S_{zz}(\mathbf{k})$  as well as its standard deviation shown as error bars in Figs. 2(a) and (b). It is apparent that  $S_{zz}(\mathbf{k})$  of the ionic fluid is sensitive to density changes only for very low packing fractions  $\eta$ . The slightly more pronounced oscillations of  $S_{zz}(\mathbf{k})$  within the DM (Fig. 2(b)) as compared to those within the RPM (Fig. 2(a)) are perhaps an artifact of the DM, within which two charged hard spheres are kept exactly at a distance  $\sigma$ , whereas the principal peak of the cation-anion pair distribution function within the RPM has a finite width [30].

Using Eq. (4), Fig. 3 displays the inverse dielectric functions  $1/\varepsilon(\mathbf{k})$  of the RPM and of the DM. The perfect screening condition [15, 22] implies  $1/\varepsilon(\mathbf{k}) \rightarrow 0$  for  $\mathbf{k} \rightarrow 0$  for an ionic fluid due to the asymptotic behavior of the charge-charge structure factor [22]

$$S_{zz}(\mathbf{k}) \stackrel{\mathbf{k} \rightarrow 0}{\simeq} \frac{\mathbf{k}^2}{\kappa^2} \quad (5)$$

with the Debye length  $1/\kappa$  being given by  $\kappa^2 = 4\pi l_B N/V$ , which is shown in the insets of Figs. 3(c) and 3(d). Unfortunately, the error bars of the three leftmost data points for  $\eta = 0.23$  (Fig. 3(c)) and of the four leftmost data points for  $\eta = 0.3$  (Fig. 3(d)) in the plots of the inverse dielectric function  $1/\varepsilon(\mathbf{k})$  of the RPM are too large to conclusively infer the functional form in the long range limit  $\mathbf{k} \rightarrow 0$  at these packing fractions. However the error bars of the RPM data in the interesting range of medium and short separations,  $|\mathbf{k}|\sigma \gtrsim 2\pi$ , and of the DM data are small. Since the DM can exhibit only orientation polarization, its dielectric function  $\varepsilon(\mathbf{k} \rightarrow 0)$  approaches a finite value of the “dielectric constant”  $\varepsilon(0)$ , which increases upon increasing the packing fraction  $\eta$  (see Fig. 3).

In order to determine the dominant polarization mechanism in an ionic fluid the inverse dielectric functions  $1/\varepsilon(\mathbf{k})$  of the RPM and of the DM in Fig. 3 are converted into the electric susceptibilities  $\chi(\mathbf{k}) = \varepsilon(\mathbf{k}) - 1$ . Figure 4 shows that the electric susceptibility  $\chi^{\text{RPM}}(\mathbf{k}) = \chi_{\text{ori}}^{\text{RPM}}(\mathbf{k}) + \chi_{\text{dis}}^{\text{RPM}}(\mathbf{k})$  of the RPM, which comprises a contribution  $\chi_{\text{ori}}^{\text{RPM}}(\mathbf{k})$  due to orientation polarization and a contribution  $\chi_{\text{dis}}^{\text{RPM}}(\mathbf{k})$  due to distortion polarization, almost coincides in the range  $|\mathbf{k}|\sigma \gtrsim 2\pi$  with the electric susceptibility  $\chi^{\text{DM}}(\mathbf{k}) = \chi_{\text{ori}}^{\text{DM}}(\mathbf{k})$  of the DM, which, by construction, exhibits only orientation polarization with susceptibility  $\chi_{\text{ori}}^{\text{DM}}(\mathbf{k})$ . Since for sufficiently large packing fractions  $\eta$  it can be expected that the orientation susceptibility  $\chi_{\text{ori}}^{\text{RPM}}(\mathbf{k})$  of the RPM is identical to the electric susceptibility  $\chi_{\text{ori}}^{\text{DM}}(\mathbf{k})$  of the DM, i.e.,  $\chi_{\text{ori}}^{\text{RPM}}(\mathbf{k}) = \chi_{\text{ori}}^{\text{DM}}(\mathbf{k})$  for all wavenumbers  $\mathbf{k}$ , one can infer the orientation and the distortion susceptibility of the RPM separately:

$$\begin{aligned} \chi_{\text{ori}}^{\text{RPM}}(\mathbf{k}) &= \chi^{\text{DM}}(\mathbf{k}), \\ \chi_{\text{dis}}^{\text{RPM}}(\mathbf{k}) &= \chi^{\text{RPM}}(\mathbf{k}) - \chi^{\text{DM}}(\mathbf{k}). \end{aligned} \quad (6)$$

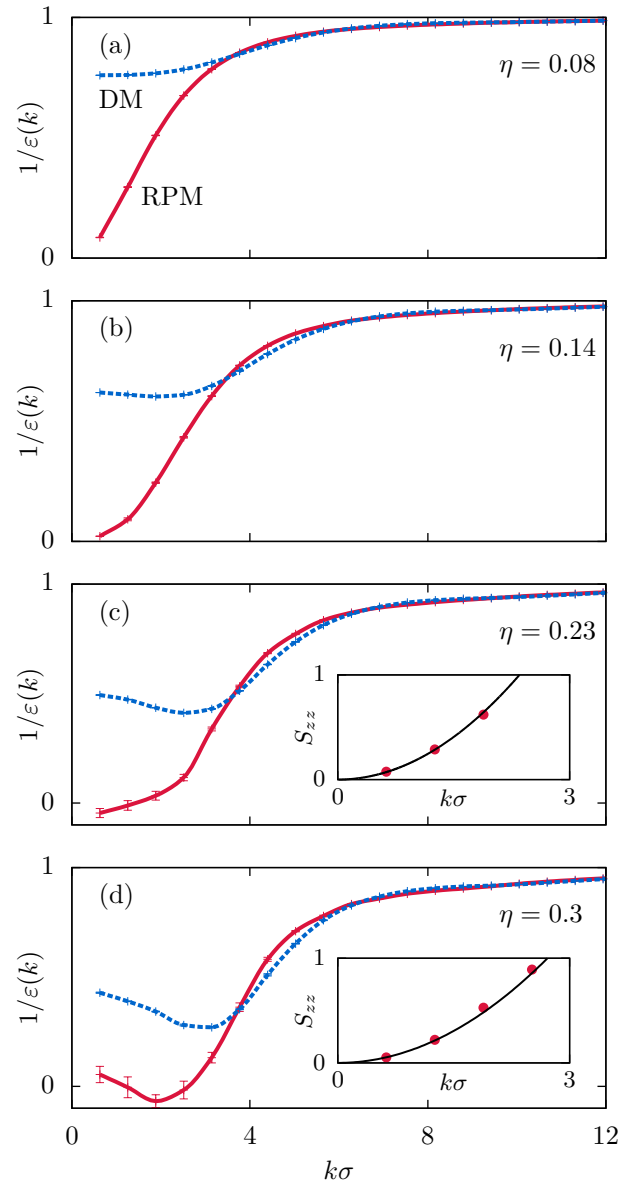


FIG. 3. Inverse dielectric functions  $1/\varepsilon(\mathbf{k})$  of the RPM ionic fluid (red solid lines, see Sec. II A) and of the DM dipolar fluid (blue dashed lines, see Sec. II A) at temperature  $T^* = 1$  and packing fractions  $\eta \in \{0.08, 0.14, 0.23, 0.3\}$ . Whereas  $1/\varepsilon(\mathbf{k} \rightarrow 0)$  becomes small (i.e.,  $\varepsilon(\mathbf{k} \rightarrow 0)$  becomes large) for the ionic fluid, the dielectric function of the dipolar fluid approaches a finite value  $\varepsilon(0)$  for small wavenumbers. The inset in panels (c) and (d) compares the charge-charge structure factor  $S_{zz}(\mathbf{k})$  obtained by means of Monte Carlo simulations (red circles) with the asymptotic behavior Eq. (5) (black solid line).

Figure 5 clearly indicates that, at  $T^* = 1$ , orientation polarization is the dominant mechanism of the RPM at sufficiently large wave numbers  $\mathbf{k}$ , whereas distortion polarization is dominating at sufficiently small wave numbers  $\mathbf{k}$ . The weak distortion polarization, i.e.,  $\chi_{\text{dis}}^{\text{RPM}}(\mathbf{k}) \approx 0$  at large wave numbers  $\mathbf{k}$  (see Fig. 5) can be

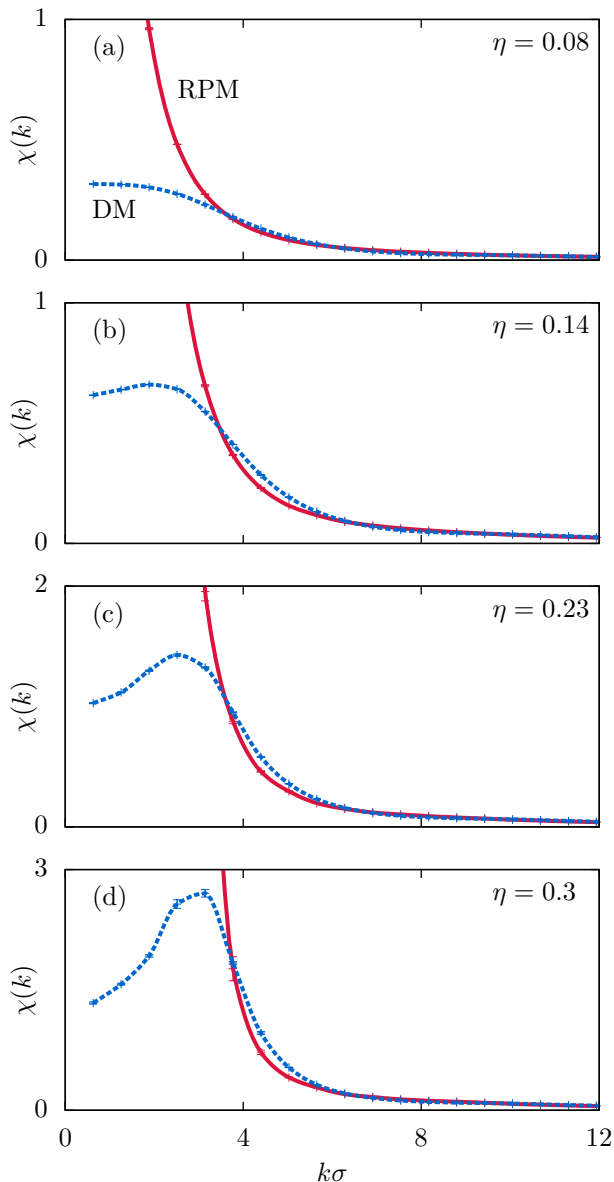


FIG. 4. Electric susceptibility  $\chi(\mathbf{k}) = \varepsilon(\mathbf{k}) - 1$  of the RPM ionic fluid (red solid lines, see Sec. II A) and of the DM dipolar fluid (blue dashed lines, see Sec. II A) at temperature  $T^* = 1$  and packing fractions  $\eta \in \{0.08, 0.14, 0.23, 0.3\}$ . Whereas  $\chi(\mathbf{k} \rightarrow 0)$  diverges for the ionic fluid due to the perfect screening of the external charges, the susceptibility of the dipolar fluid approaches a finite value  $\chi(0)$  for small wavenumbers. At large wavenumbers  $|\mathbf{k}|\sigma \gtrsim 2\pi$  the electric susceptibility  $\chi(\mathbf{k}) = \chi_{\text{ori}}(\mathbf{k}) + \chi_{\text{dis}}(\mathbf{k})$  of the RPM almost coincides with that of the DM, which, by construction, possesses only orientation polarization whose electric susceptibility can be expected to be close to  $\chi_{\text{ori}}(\mathbf{k})$  of the RPM (see Sec. II A).

attributed to the impenetrable hard cores of the ions of the RPM. The crossover wavenumber between distortion-dominated and orientation-dominated polarization increases with packing fraction  $\eta$ . There is a certain interval of wavenumbers  $|\mathbf{k}|\sigma \approx 4 \dots 5$  with  $\chi_{\text{dis}}^{\text{RPM}}(\mathbf{k}) < 0$  (see

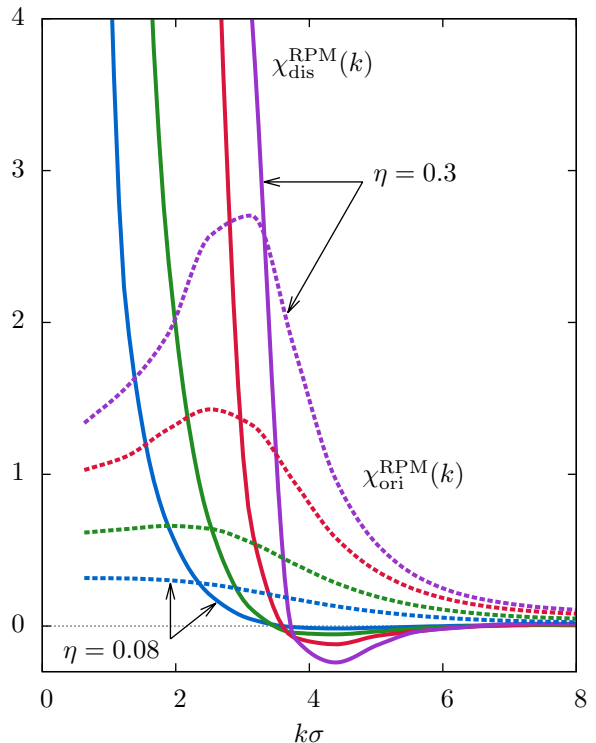


FIG. 5. Distortion susceptibilities  $\chi_{\text{dis}}^{\text{RPM}}(\mathbf{k})$  (solid lines) and orientation susceptibilities  $\chi_{\text{ori}}^{\text{RPM}}(\mathbf{k})$  (dashed lines) of the RPM at temperature  $T^* = 1$  for packing fractions  $\eta \in \{0.08, 0.14, 0.23, 0.3\}$ . Perfect screening corresponds to the divergence of  $\chi_{\text{dis}}^{\text{RPM}}(\mathbf{k})$  in the long wavelength limit  $|\mathbf{k}| \rightarrow 0$ . The region of negative distortion susceptibility,  $\chi_{\text{dis}}^{\text{RPM}}(\mathbf{k}) < 0$ , can be interpreted as overscreening. At sufficiently large wave numbers orientation polarization dominates over distortion polarization with the crossover wave numbers increasing with the packing fraction  $\eta$  (see Fig. 6).

Fig. 5), which indicates overscreening, which is caused by steric effects, i.e., by the hard ion cores, too. The distortion susceptibility of the RPM diverges for  $\mathbf{k} \rightarrow 0$  according to  $\chi_{\text{dis}}^{\text{RPM}}(\mathbf{k}) \sim 1/k^2$ , which corresponds to the perfect screening property of plasmas [15, 22]. Hence, it has been shown here, that the RPM ionic fluid exhibits dielectric properties similar to a dipolar fluid at short range, whereas it behaves plasma-like at long range.

Figure 6 displays the crossover wave numbers  $k^\times(\eta, T^*)\sigma$  (dots  $\bullet$ ), defined by equal orientation and distortion susceptibilities,  $\chi_{\text{ori}}^{\text{RPM}}(k^\times) = \chi_{\text{dis}}^{\text{RPM}}(k^\times)$ , as functions of the packing fraction  $\eta$  and of the temperature  $T^*$ . The RPM exhibits plasma-like behavior for  $k < k^\times(\eta, T^*)$  and dipolar-fluid-like behavior for  $k > k^\times(\eta, T^*)$ . The general trend is that of increasing values of  $k^\times(\eta, T^*)\sigma$  upon increasing the packing fraction  $\eta$  or decreasing the temperature  $T^*$ . However, it can be expected that  $k^\times(\eta, T^*) < 2\pi/\sigma$  for any set of parameters  $(\eta, T^*)$  since an external electric field oscillating with a wave length equal to the ion diameter  $\sigma$  (see the thin vertical dashed line in Fig. 6) cannot lead to distortion po-



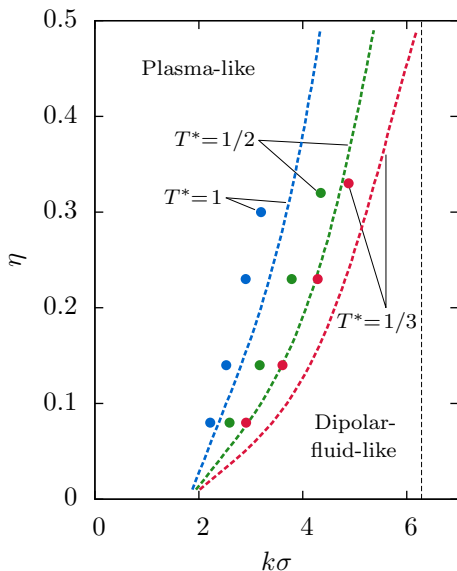


FIG. 6. Crossover wave numbers  $k^\times(\eta, T^*)\sigma$  of the RPM between plasma-like behavior for  $k < k^\times(\eta, T^*)$  and dipolar-fluid-like behavior for  $k > k^\times(\eta, T^*)$  as functions of the packing fraction  $\eta$  and of the temperature  $T^*$ . The crossover wave number  $k^\times(\eta, T^*)$  is defined by equal orientation and distortion susceptibilities,  $\chi_{\text{ori}}^{\text{RPM}}(k^\times) = \chi_{\text{dis}}^{\text{RPM}}(k^\times)$  (see Eq. (6)). The dots (•) correspond to simulation data whereas the dashed lines are obtained by means of the simple approximate calculation described in the main text. The latter captures the correct trends of increasing values  $k^\times(\eta, T^*)\sigma$  upon increasing the packing fraction  $\eta$  or decreasing the temperature  $T^*$ . The thin vertical dashed line marks  $k\sigma = 2\pi$ , which corresponds to an upper bound of  $k^\times(\eta, T^*)\sigma$ .

larization, i.e., the crossover  $\chi_{\text{ori}}^{\text{RPM}}(k^\times) = \chi_{\text{dis}}^{\text{RPM}}(k^\times)$  has to occur at some smaller wave number. The dashed lines in Fig. 6 correspond to an approximation of  $k^\times(\eta, T^*)\sigma$  with  $\chi^{\text{RPM}}(\mathbf{k})$  in Eq. (6) being approximated within the mean spherical approximation (MSA) of the RPM [22] and with  $\chi^{\text{DM}}(\mathbf{k})$  in Eq. (6) being approximated by the expression of a single dumbbell particle in an external electric field. Whereas this simple approximation slightly overestimates the value of  $k^\times(\eta, T^*)\sigma$ , the general trends of increasing values of  $k^\times(\eta, T^*)\sigma$  upon increasing the packing fraction  $\eta$  or decreasing the temperature  $T^*$  are captured correctly. Hence for dense ionic fluids, e.g., inorganic fused salts ( $\eta \approx 0.5, T^* \approx 1/30$ ) or RTILs ( $\eta \approx 0.5, T^* \approx 1/50$ ), one can expect plasma-like behavior in a very wide range of wave numbers  $k < k^\times$  with  $2\pi/k^\times$  corresponding almost to the size of the ions.

#### IV. CONCLUSIONS

The main observation of the previous Sec. III, that the RPM ionic fluids exhibits dielectric properties simi-

lar to a dipolar fluid at short range whereas it behaves plasma-like at long range, does not hinge on any peculiar property of the RPM and can hence be expected to be made for other ionic fluids, too. Moreover, our approach in Sec. III to decompose the electric susceptibility  $\chi(\mathbf{k}) = \chi_{\text{ori}}(\mathbf{k}) + \chi_{\text{dis}}(\mathbf{k})$  into a contribution  $\chi_{\text{ori}}(\mathbf{k})$  due to orientation polarization and a contribution  $\chi_{\text{dis}}(\mathbf{k})$  due to distortion polarization by introducing a corresponding dipolar fluid made of cation-anion compounds applies to the case of other ionic fluids, too. In general, the structure of the cation-anion compounds comprising the dipolar fluid corresponding to an ionic fluid can be conjectured on the basis of, e.g., the pair distribution function, which is routinely calculated for numerous ionic fluid models (see, e.g., Ref. [31, 32]). Hence, the method described in Sec. III could be a useful tool to assess the bulk dielectric properties of general ionic fluid models.

The results of Sec. III are restricted to bulk ionic fluids and they cannot be applied quantitatively in the context of the discussion on the interpretation of SFA measurements in an RTIL environment [9–11], which is related to confined ionic fluids. The reason for this restriction is that the static dielectric function for non-uniform systems is of the form  $\varepsilon(\mathbf{k}, \mathbf{k}')$  due to the absence of translational symmetry. However, the qualitative picture occurring in Sec. III suggests, that strongly confined ionic fluids tend to behave as dipolar fluids whereas they progressively exhibit plasma-like properties upon relaxing the confinement. This suggests that the recently debated interpretation of RTILs as dilute electrolyte solutions [9, 12] might not be simply a yes-no-question but it might depend on the considered length scale.

The finding in Sec. III, that the static dielectric properties of ionic fluids depend on the length scale, may be considered complementary to the observation that the quantification of the polarity of RTILs depends on the intrinsic time scale of the measurement [20].

In summary, based on grandcanonical Monte Carlo simulations of the restricted primitive model and a corresponding dumbbell model, it has been argued that bulk ionic fluids at small length scales are expected to behave as dipolar fluids, for which orientation polarization dominates, whereas at large length scales plasma-like behavior occurs, for which distortion polarization dominates. In the style of Ref. [20], one can conclude that the static dielectric properties of ionic fluids depend on the length scale on which they are looked at.

- 
- [1] G.J. Janz, *Molten salts handbook* (Academic Press, New York, 1967).
- [2] P. Walden, Bull. Acad. Imp. Sci. St.-Petersbourg **1914**, 405.
- [3] H. Weingärtner, Ang. Chem. Int. Ed. **47**, 654 (2008).
- [4] D.H. Zaitsau, G.J. Kabo, A.A. Strechan, Y.U. Paulechka, A. Tschersich, S.P. Verevkin, and A. Heintz, J. Phys. Chem. A **110**, 7303 (2006).
- [5] M. Bier and S. Dietrich, Mol. Phys. **108**, 211 (2010).
- [6] D.R. Macfarlane, J. Golding, S. Forsyth, Maria Forsyth, and G.B. Deacon, Chem. Commun., 1430 (2001).
- [7] K.R. Seddon, A. Stark, and M.-J. Torres, Am. Chem. Soc. Symp. Ser. **819**, 34 (2002).
- [8] P.A. Hunt, Mol. Sim. **32**, 1 (2006).
- [9] M.A. Gebbie, M. Valtiner, X. Banquy, E.T. Fox, W.A. Henderson, and J.N. Israelachvili, Proc. Nat. Acad. Sci. USA **110**, 9674 (2013).
- [10] S. Perkin, M. Salanne, P. Madden, and R. Lynden-Bell, Proc. Nat. Acad. Sci. USA **110**, E4121 (2013).
- [11] M.A. Gebbie, M. Valtiner, X. Banquy, W.A. Henderson, and J.N. Israelachvili, Proc. Nat. Acad. Sci. USA **110**, E4122 (2013).
- [12] A.A. Lee, D. Vella, S. Perkin, and A. Goriely, J. Phys. Chem. Lett. **6**, 159 (2015).
- [13] R.D. Bezman, E.F. Casassa and R.L. Kay, J. Mol. Liq. **73**, 397 (1997).
- [14] M. Mohsen-Nia and H. Amiri, J. Chem. Thermod. **57**, 67 (2013).
- [15] F. Stillinger and R. Lovett, J. Chem. Phys. **49**, 1991 (1968).
- [16] J.-P. Hansen and I.R. McDonald, Phys. Rev. A **11**(6), 2111 (1975).
- [17] H. Weingärtner, A. Knocks, W. Schrader, and U. Kaatze, J. Phys. Chem. A **105**, 8646 (2001).
- [18] H. Weingärtner, Z. Phys. Chem. **220**, 1395 (2006).
- [19] C. Dagueneat, P.J. Dyson, I. Krossing, A. Oleinikova, J. Slattery, Ch. Wakai, and H. Weingärtner, J. Phys. Chem. B **110**, 12682 (2006).
- [20] M.Y. Lui, L. Crowhurst, J.P. Hallett, P.A. Hunt, H. Hiedermeyer, and T. Welton, Chem. Sci. **2**, 1491 (2011).
- [21] P.W. Atkins, *Physical chemistry* (Oxford University Press, Oxford, 1998).
- [22] J.-P. Hansen and I.R. McDonald, *Theory of simple liquids* (Elsevier, Amsterdam, 2008).
- [23] N. Metropolis, A.W. Rosenbluth, M.N. Rosenbluth, A.H. Teller, and E. Teller, J. Chem. Phys. **21**, 1087 (1953).
- [24] M.P. Allen and D.J. Tildesley, *Computer simulation of liquids* (Clarendon Press, Oxford, 1987).
- [25] D. Frenkel and B. Smit, *Understanding molecular simulation: from algorithms to applications* (Academic Press, San Diego, 2002).
- [26] P.P. Ewald, Ann. Physik **369**, 253 (1921).
- [27] A. Arnold, O. Lenz, S. Kesselheim, R. Weeber, F. Fahrenberger, D. Roehm, P. Košovan and C. Holm, in *Lecture notes in computational science and engineering*, Vol. 89, edited by M. Griebel and M.A. Schweitzer (Springer, , 2013), p. 1.
- [28] H.-J. Limbach, A. Arnold, B.A. Mann and C. Holm, Comput. Phys. Commun. **174**, 704 (2006).
- [29] M.E. Fisher, J. Stat. Phys. **75**, 1 (1994).
- [30] We are indebted to Yu.V. Kalyuzhnyi for this comment.
- [31] F. Dommert, K. Wendler, B. Qiao, L. Delle Site and C. Holm, J. Mol. Liq. **192**, 32 (2014).
- [32] A. Pádua, M. Costa Gomes and J. Canongia Lopes, Acc. Chem. Res. **40**, 1087 (2007).